Solar Activity Monitoring and Forecasting

Peter Gallagher
University College Dublin
&
NASA Goddard Space Flight Center

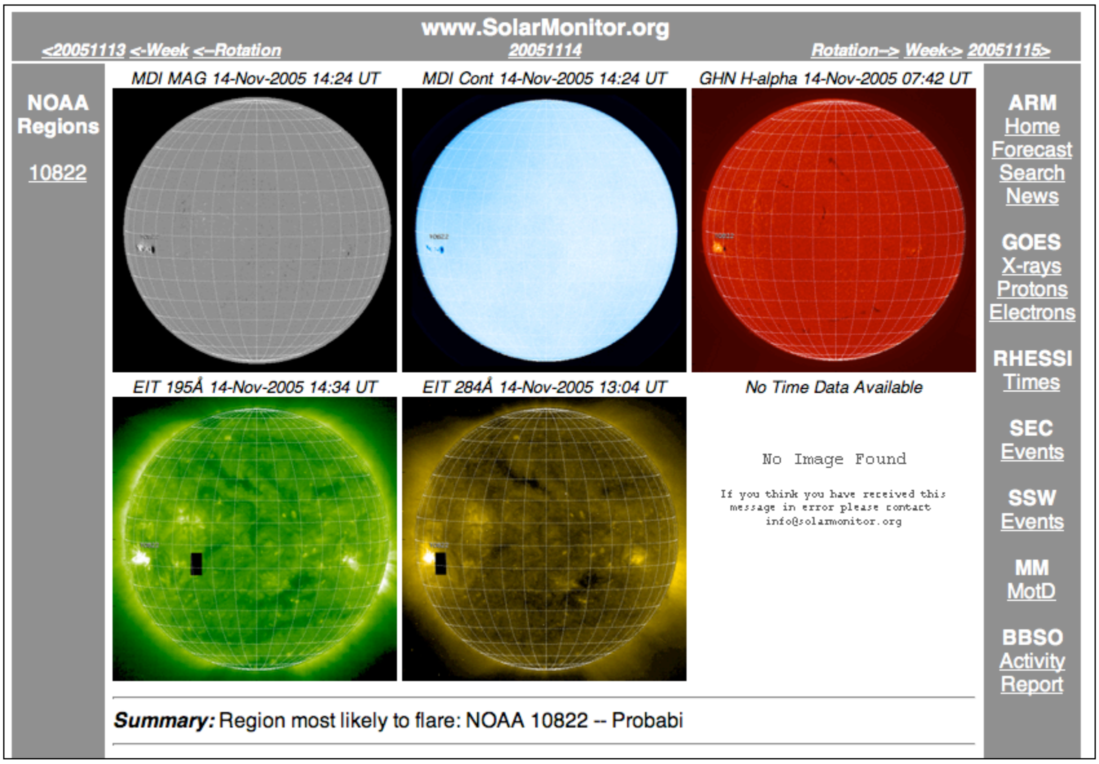

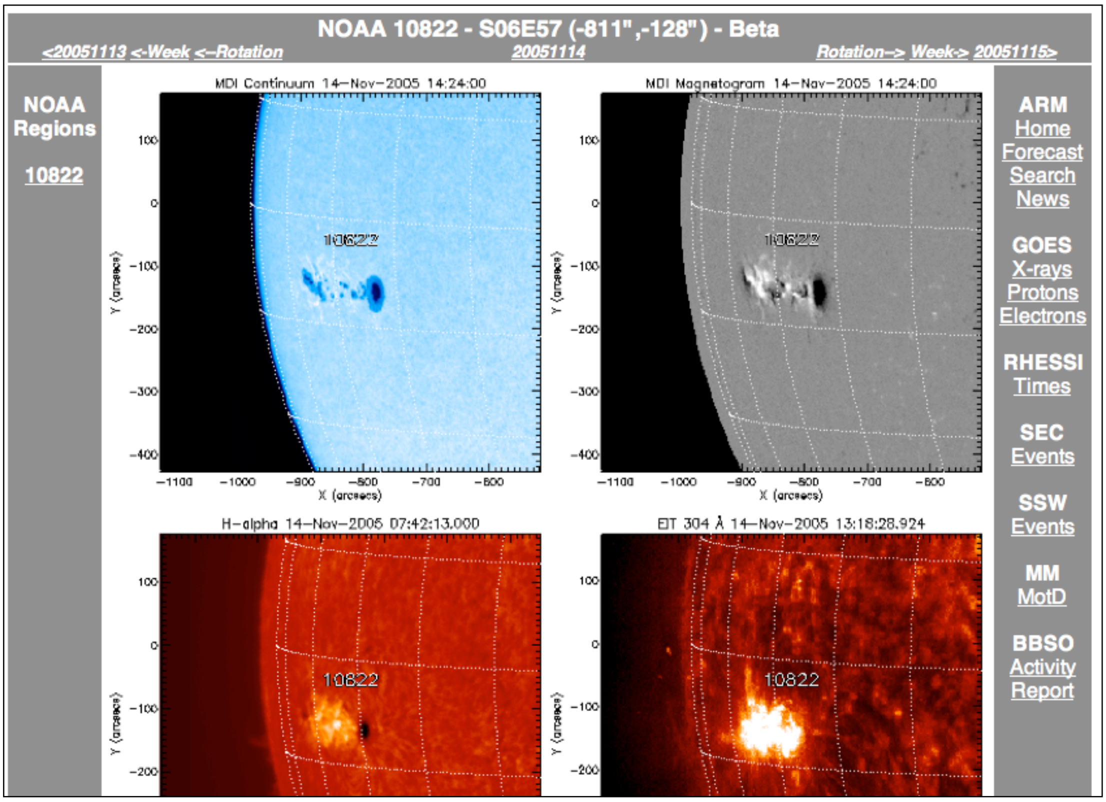

GONG+ Magnetogram | MDI Magnetogram | MDI Continuum | GHN H-alpha | EIT 304 Å | EIT 171 Å | EIT 195 Å | EIT 284 Å | SXI X-rays | Fulldisk Slideshow

Today's NOAA Active Regions

Number	Location	Hale	McIntosh	Area	NSpots	Events
10822	S06E57 (-811",-128")	β/α	Cao/Hsx	0120/0120	06/01	C2.0(00:19) C1.4(01:49) C7.3(03:55) C1.0(05:47) C2.8(08:30) C1.0(11:44) M2.6(04:16) M3.9(14:16) /C9.5(00:13) C1.9(03:09) C6.7(04:28) C2.7(06:00) C3.0(06:53) C2.7(12:41) C2.8(21:19) M2.5(14:29)

Events not associated with currently named NOAA regions: None

Note: The tabulated data are based on the most recent NOAA/USAF Active Region Summary issued on 14-Nov-2005 00:30 UT , the values to the right of the forward slashes representing yesterdays values or events. The region positions are valid on 14-Nov-2005 15:30 UT .

Web Curators: *Peter T. Gallagher, Russ Hewett, James McAteer - info@solarmonitor.org*
Webmaster: *Amy E. Skowronek*
Responsible NASA official: *Joseph B. Gurman*
NASA security and privacy protection statement

These pages are automatically updated every 30 minutes.
Last updated: 14-Nov-2005 15:30 UT

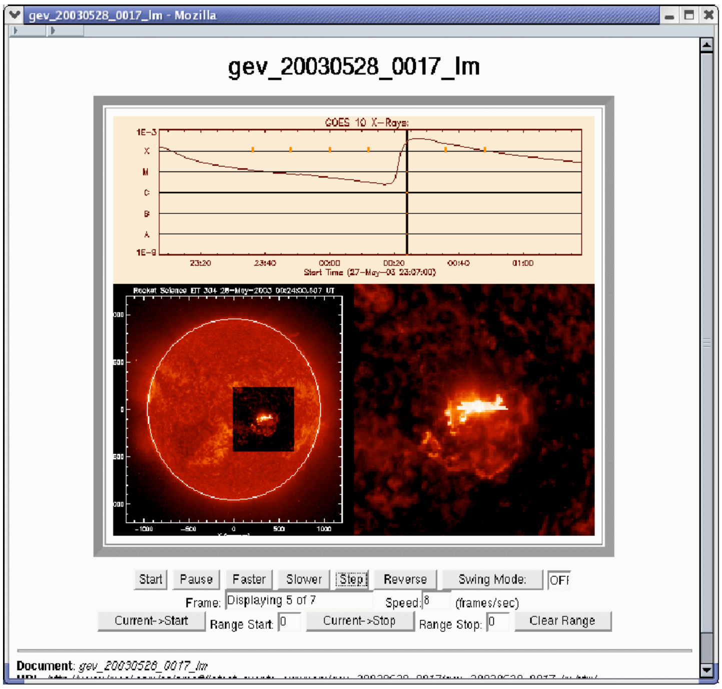

Mount Wilson α Region

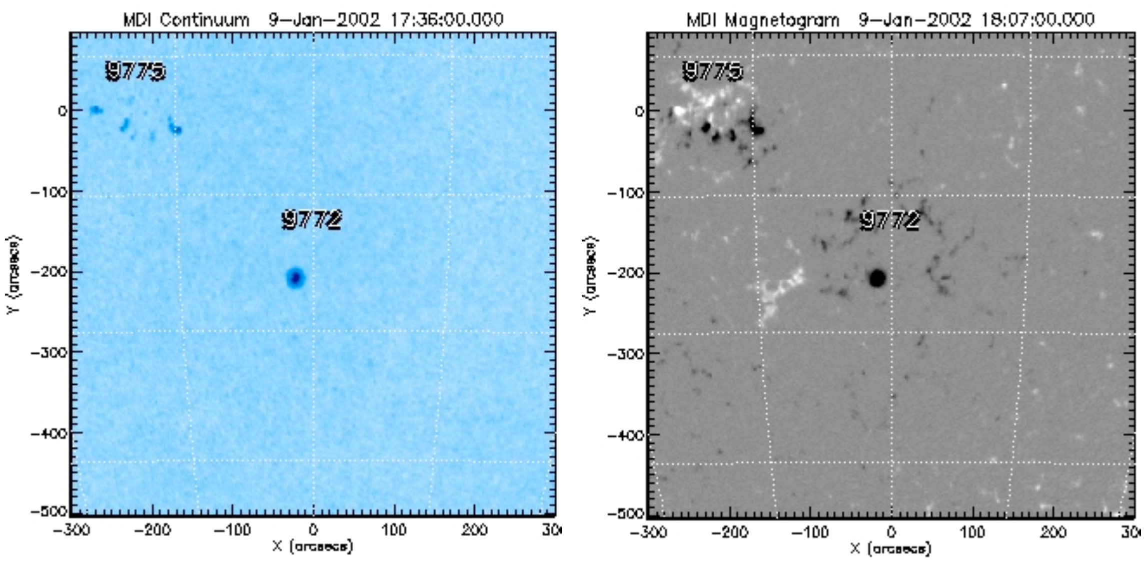

Mount Wilson β Region

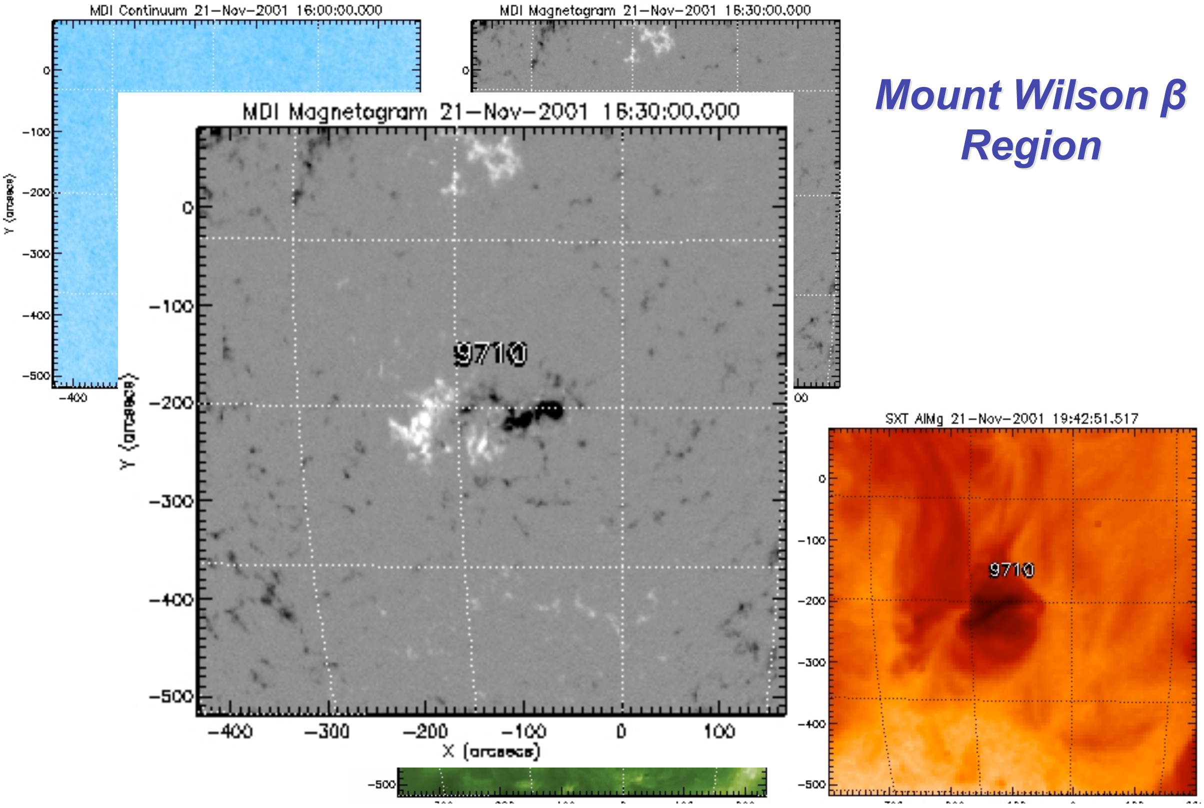

Mount Wilson βγδ Region

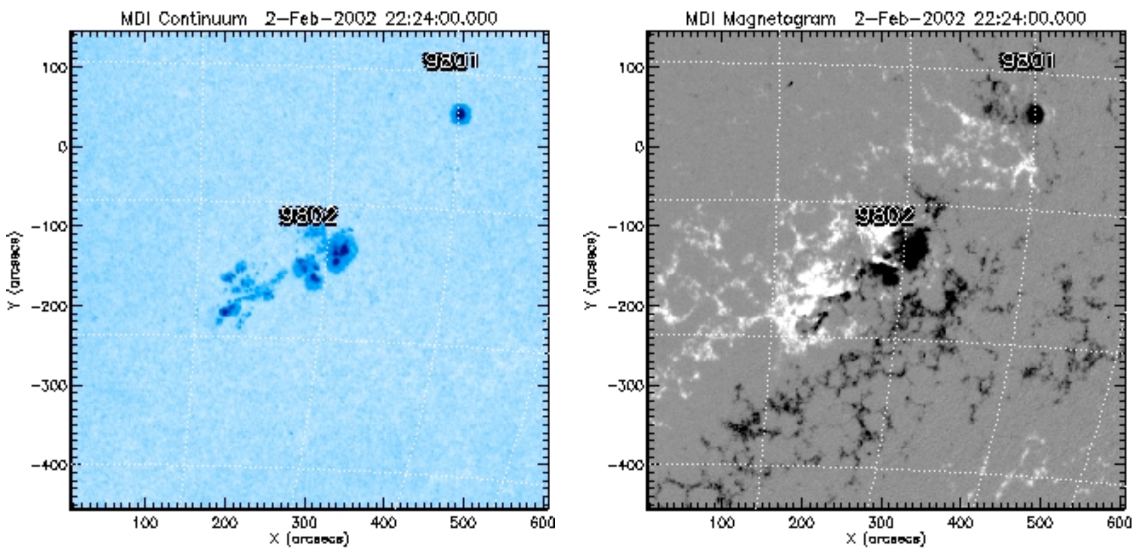

Active Region Characterisation

Include measures that are physically motivated and that give a measure of energy storage/release:

- **Fractal dimension:** relates to the active region complexity.
- **Field gradient:** indicative of energy build-up in the photosphere.
- **Neutral lines:** related to energy release locations.
- **Emerging flux regions:** can act as energy release triggers.
- **Wavelet analysis:** diagnostic of small and large scale morphology.

Fractal Dimension - Motivation

- Turbulent plasma motions => fields follow a random walk.
- Percolation theory: geometry of flux concentrations on the solar surface naturally result in fractals (Vlahos et al., 2002; Schrijver et al., 1992; Seiden & Wentzel, 1996).
- Magnetic fields scale in a self-similar and fractal manner.
  - Correlation between Mt. Wilson classification and fractal dimension (McAteer, Gallagher, et al., ApJ 2005).
- Measuring the fractal dimension of an active region magnetic field is an essentially global investigation of the scaling properties of the magnetic field.

Fractal Dimension - Methods

- **Box-Counting Dimension** (Mandelbrot):

$$N(\varepsilon) = \varepsilon^{-\delta_{BC}}$$

  - The box-counting dimension can then be then determined from the slope,

$$\delta_{BC} = \frac{\log(N(\varepsilon))}{\log(1/\varepsilon)}$$

- **Perimeter-Area Dimension** (Hausdorff):

$$P = A^{\delta_{PA}/2}$$

  - The perimeter-area dimension can then be obtained from,

$$\delta_{PA} = 2\frac{\log(P)}{\log(A)}$$

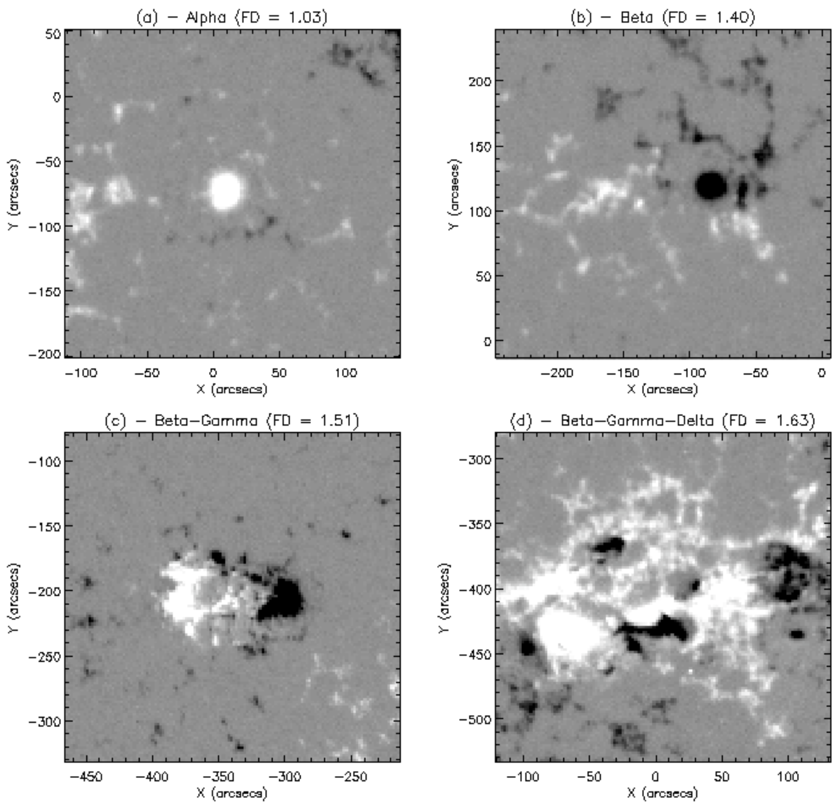

Fractal Dimension - Example

- $\alpha \sim 1.0 - 1.2$
- $\beta \sim 1.2 - 1.4$
- $\beta\gamma \sim 1.4 - 1.6$
- $\beta\gamma\delta \sim 1.5 - 1.7$

- Error $\sim \pm 0.1$

Horizontal Gradient - Motivation

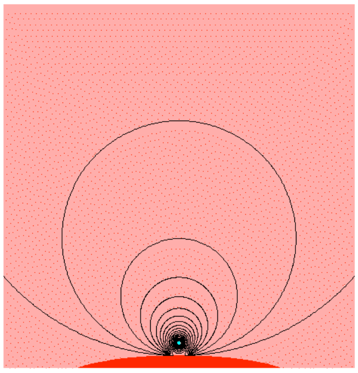

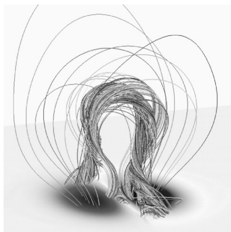

- Large transverse gradients are observed across the neutral line of large delta spots (Patty & Hagyard, 1986; Zhang et al., 1994).
- Converging photospheric flows sweep opposite polarity fields towards the neutral line of the delta.
- Over hours, continued concentration of polarities in a leads to strong transverse gradients (Gallagher, Moon, & Wang 2002).
- t_{energy_buldup} (hrs - days) >> $t_{energy\_resease}$ (secs - mins)
- An instability results in the release of stored energy (Lin & Forbes, 2001; Priest & Forbes, 1990)

Horizontal Gradient - Method

- The horizontal gradient of the line-of-sight field, $\mathbf{B}_z(x,y)$ can be calculated using,

$$\nabla_h \mathbf{B}_z(x,y) = \left(\frac{\partial \mathbf{B}_z(x,y)}{\partial x}\right)\hat{i} + \left(\frac{\partial \mathbf{B}_z(x,y)}{\partial x}\right)\hat{i}$$

- Magnitude of gradient can be evaluated using,

$$\left|\nabla_h \mathbf{B}_z(x,y)\right| = \sqrt{\left(\frac{\partial \mathbf{B}_z(x,y)}{\partial x}\right)^2 + \left(\frac{\partial \mathbf{B}_z(x,y)}{\partial x}\right)^2}$$

- While the direction can be found from,

$$\theta = \arctan\left(\frac{\partial \mathbf{B}_z(x,y)}{\partial x}, \frac{\partial \mathbf{B}_z(x,y)}{\partial y}\right)$$

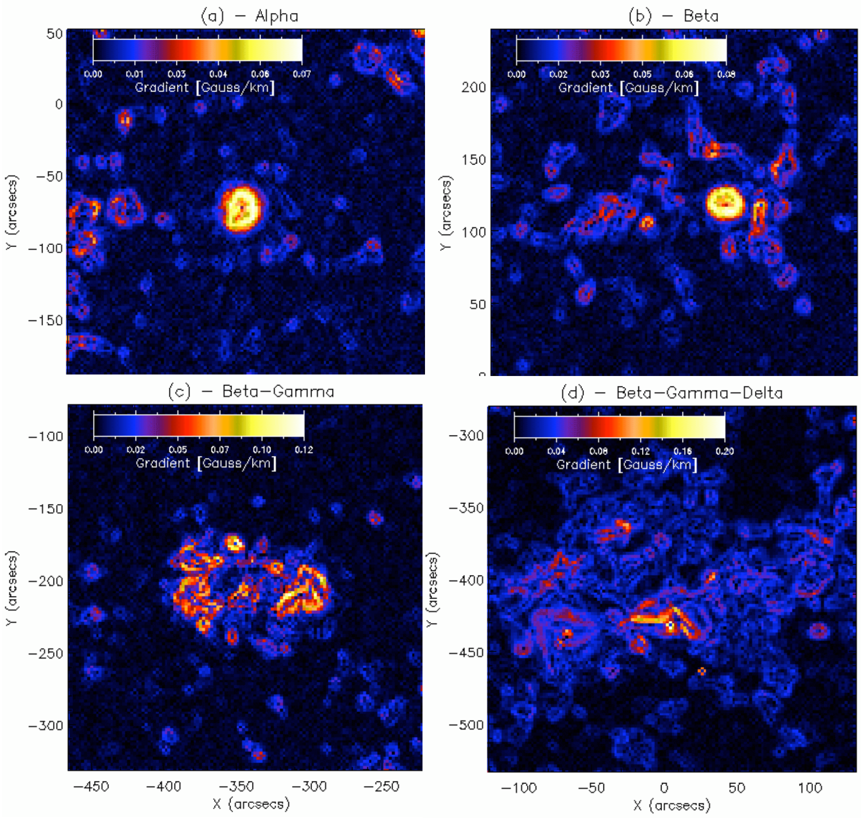

Horizontal Gradient - Example

- Gradients are large for ***large fields in close proximity.***

NOAA 10486

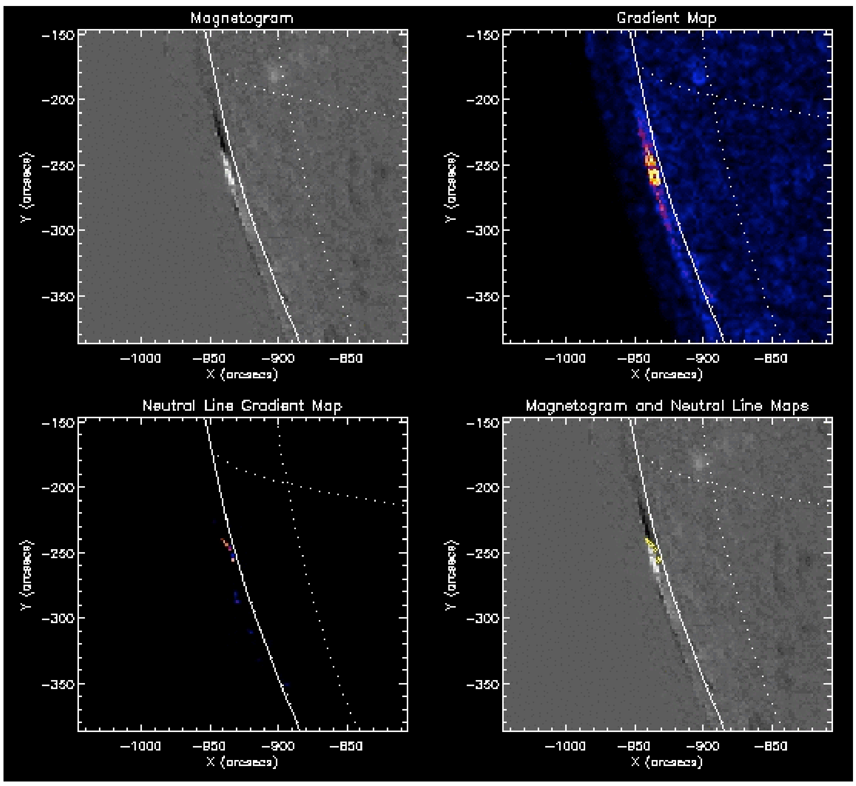

- Strong transverse gradients in B_{los}.
- Multiple long and complex neutral lines.
- X17.2 (28 Oct)
- X10.0 (29 Oct)
- X8.3 (2 Nov)

NOAA 10488

- Short neutral lines.
- Strong gradients.
- X2.7 (3 Nov).
- X3.9 (3 Nov).

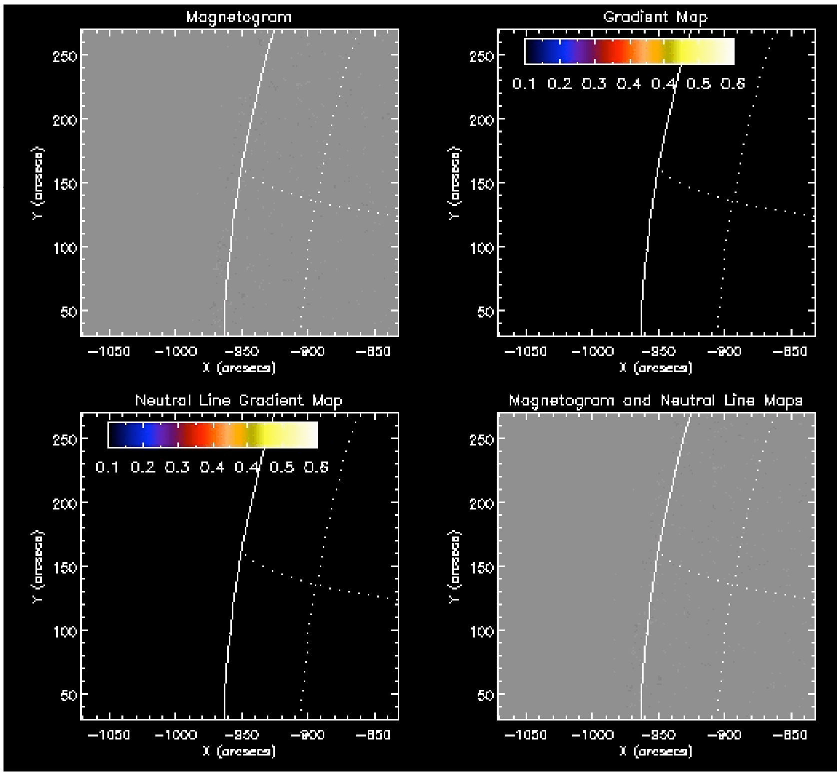

Neutral Line - Motivation

- Energy can be stored in the corona when sunspots of opposite polarity are pushed together, forming an extended current sheet above the neutral line in the overlying magnetic field (Parker, 1963; Roumeliotis & Moore, 1993).
- “Break-out” model: gradual shearing motion both across and along the neutral line, can result in the formation of unstable arcades structures in the solar corona, which can then erupt (Antiochos, Devore, & Klimchuk, 1999).
- Observational flare signatures in neutral line morphology.

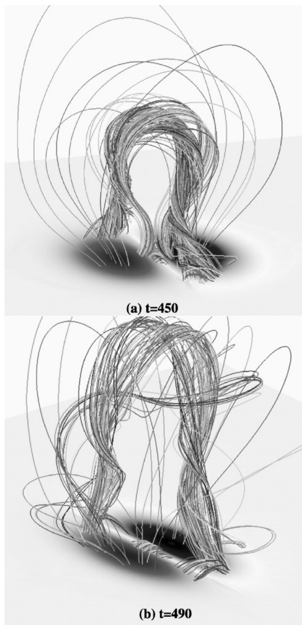

Neutral Line - Method

- Magnetogram is first **smoothed** using a boxcar filter.
- **Contours** of constant magnetic flux are then overlayed on the magnetogram at the zero Gauss level.
- Pixels along these contours are then extracted and used to create a **binary image**, with pixels along the neutral line have a value of 1, and all others being set to 0.
- This binary mask can then be used to extract **gradient values** along the neutral line by multiplying it with the gradient map.

Neutral Line - Example

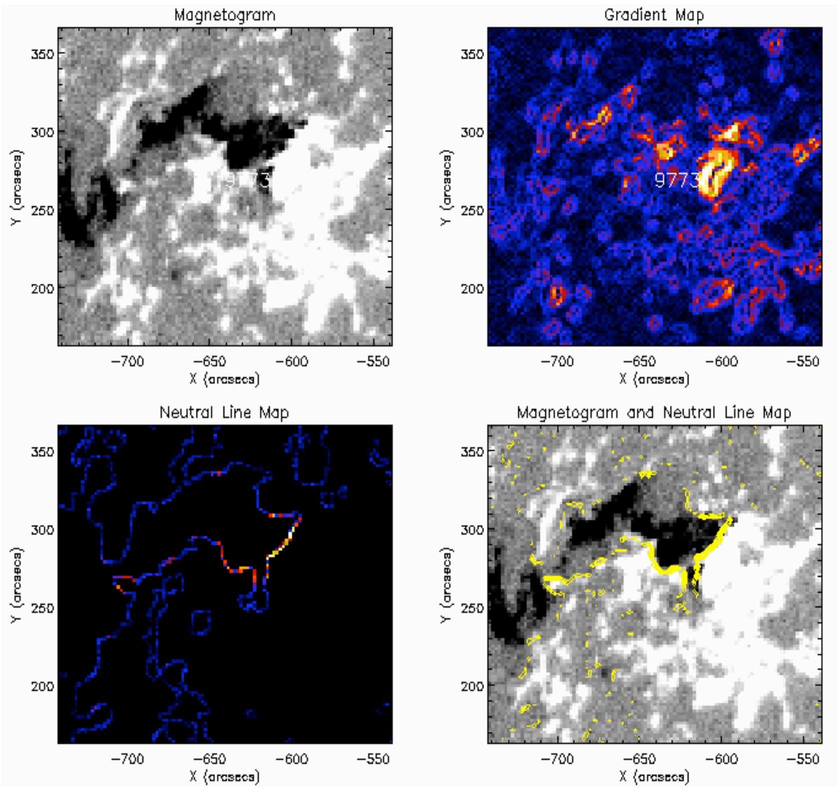

NOAA 10486

- Strong transverse gradients in B_{los}.
- Multiple long and complex neutral lines.
- X17.2 (28 Oct)
- X10.0 (29 Oct)
- X8.3 (2 Nov)

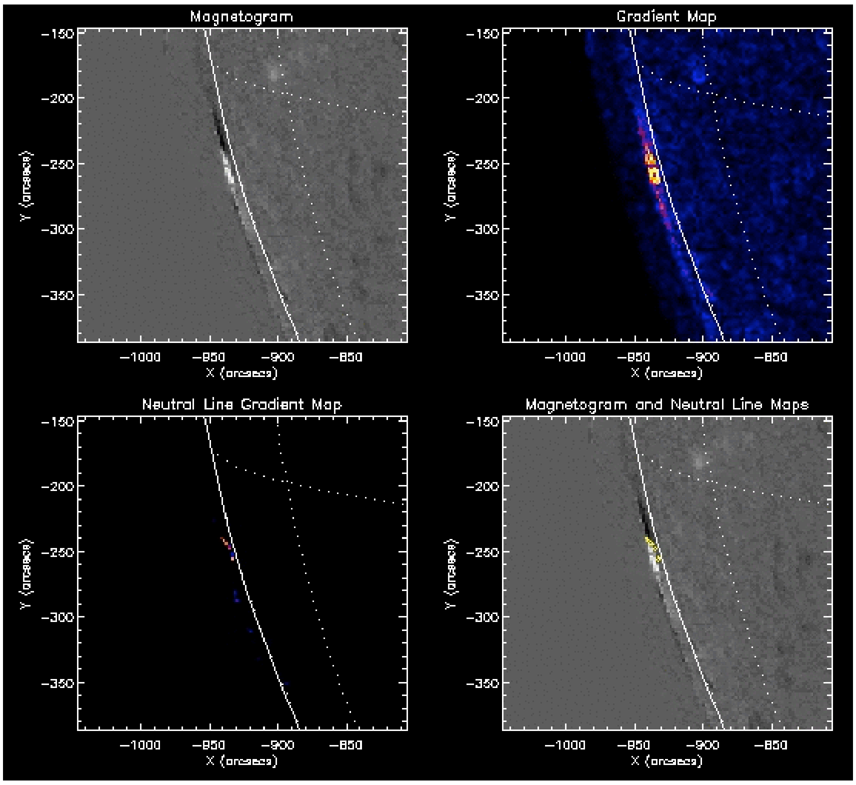

Emerging/Submerging Flux Regions (ESFRs) - Motivation

- Filament eruptions can be triggered by ESFRs (Feynman & Martin, 1995).
- Major flares tend to be associated with new flux emergence (Tang & Wang, 1993; Wang et al. 2003; Zharkova).
- CMEs, which may be associated with filament eruptions and/or flares, may also be triggered by ESFRs (Green et al., 2003).
- Emerging flux model (Heyvaerts, Priest, & Rust, 1977).
- Flux-rope destabilization by flux injection (Krall, Chen, & Santoro, 2000).

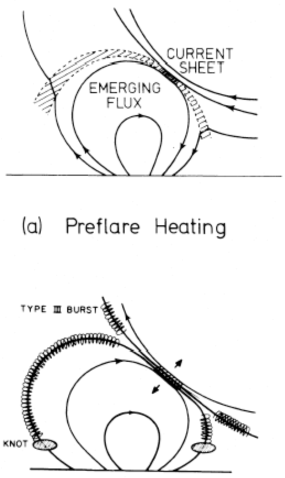

(a) Preflare Heating

(b) Impulsive Phase

Emerging/Submerging Flux Regions (ESFRs) - Method

- Automatic monitoring of ESFRs is important to tracking and predicting solar activity.
- ESFRs will be monitored using full-disk magnetograms in conjunction with a near real-time running-difference algorithm.
- Each newly processed magnetogram can be differentially rotated to the location of the previously processed magnetogram and subtracted.
- ESFRs are then identified as areas in the difference image showing large deviations above the mean difference level.
- ESFR frequency and location will then be cataloged and overplotted on images obtained at EUV or X-ray wavelengths, for example.

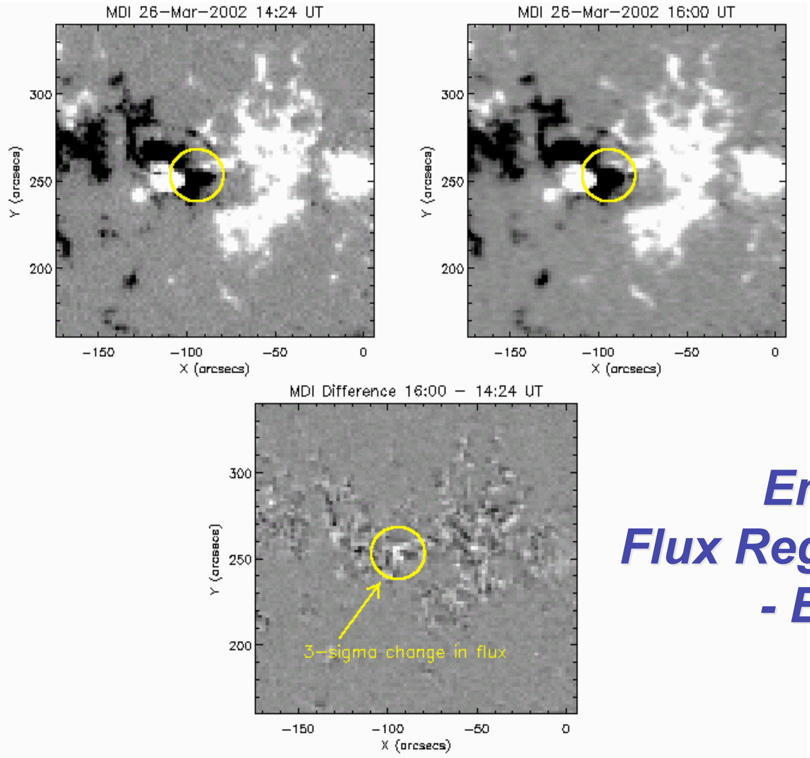

Emerging Flux Regions (ESFRs) - Example

Wavelets - Motivation

- Measuring the fractal dimension of an active region magnetic field is an essentially global investigation of the scaling properties of the magnetic field.
  - =>overlooks spatially localized scale features, such as the emergence/submergence of flux tubes.

- A wavelet analysis of magnetograms can identify such regions.

- Wavelets give distribution of length-scales => crucial for active region characterisation.

Wavelets - Method

- Test the suitability of various wavelet decomposition schemes (Haar, a trous, etc.)

- Find and characterize the local scale content of magnetograms and analyze this in the context of flare occurrence locations, times, rates and flux emergence/submergence.

- Characterize the evolution of spatial distribution of magnetogram scale content via entropy measures.

Wavelets - Example

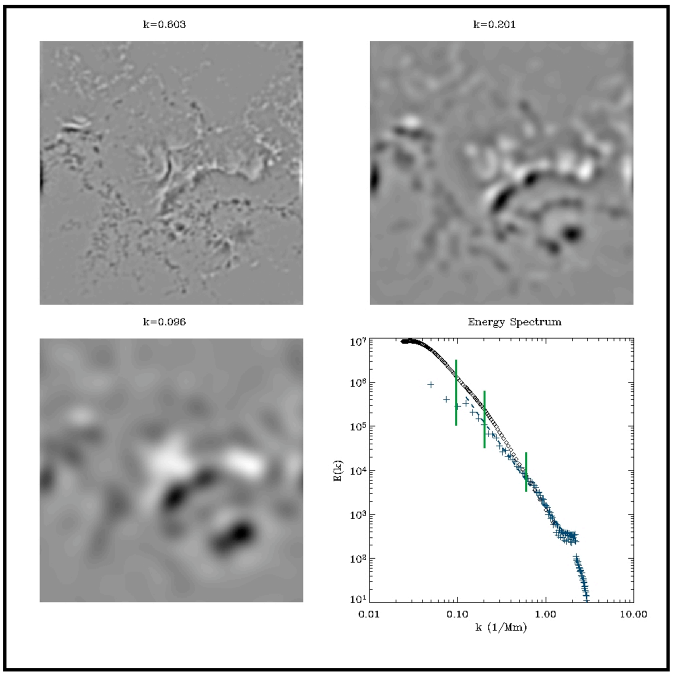

Wavelets - Example

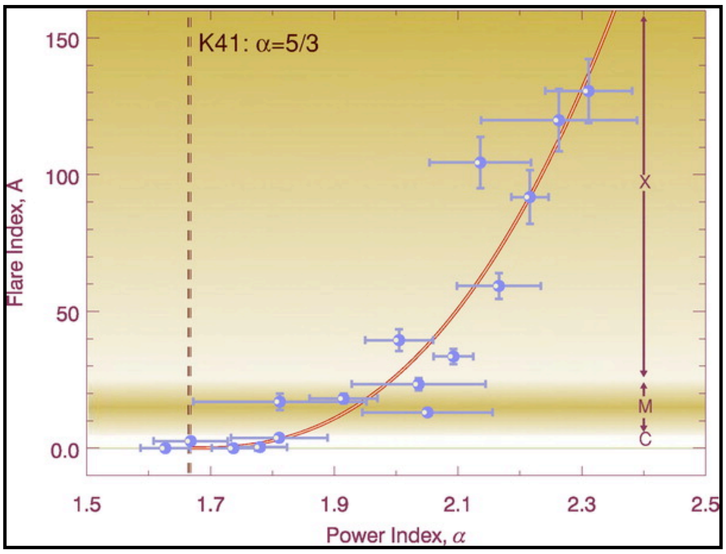

Future Directions

- *Autonomous:*
  - Operation via image processing.
- *Distributed:*
  - Essential for real-time operation in SDO, STEREO, etc era.
- *Redundant:*
  - Must be operational 24/7. Servers in US, Europe and Korea.
- *Integrated:*
  - Must connect events on the Sun to events on and near Earth/planets.

Sun-Planet Connection

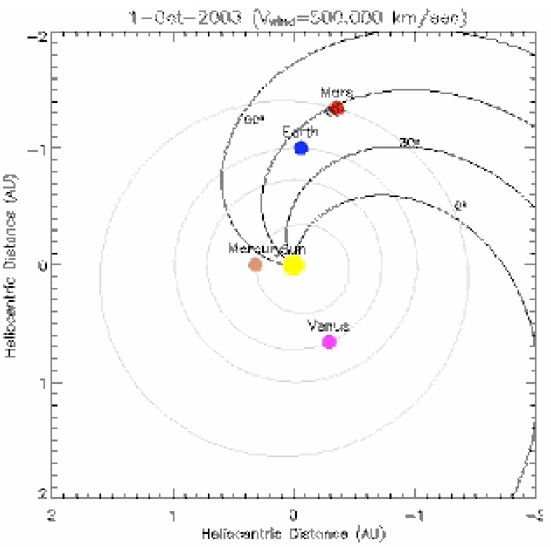

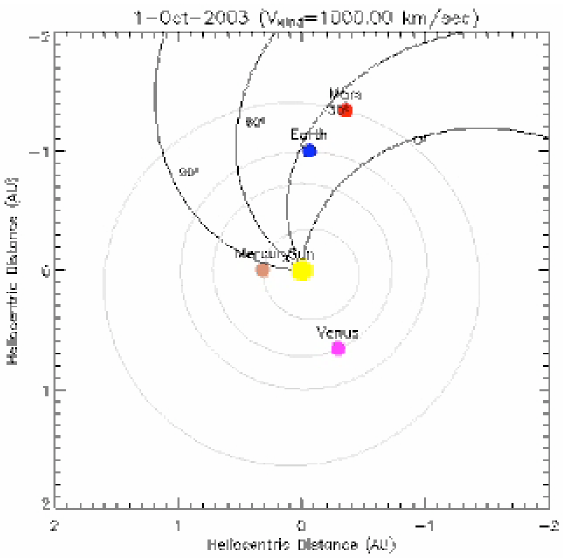

- Assume Parker spiral of form: $B_\theta = \frac{v_{SW}}{\Omega}\sin(\theta)$
- See a space weather report for Mars at http://www.solarmonitor.org/~ptg/mars

Funding

- Funded until now by NASA.
- *Imagine Technologies Ltd. (www.imagine-technologies.com)* proposal accepted by Enterprise Ireland for space weather market analysis (€40k).
- Proposal submitted to *Science Foundation Ireland* for R&D (€1M).
- No current European funding - looking to partner/collaborate with companies/researchers/agencies in Europe.

Collaborators/Thanks

- James McAteer, Jack Ireland, Alex Young, Russ Hewett
  NASA Goddard Space Flight Centre
- Paul Conlon and Claire Whelan
  University College Dublin
- COST 724 - funding to make this presentation.